



*Supplement of*

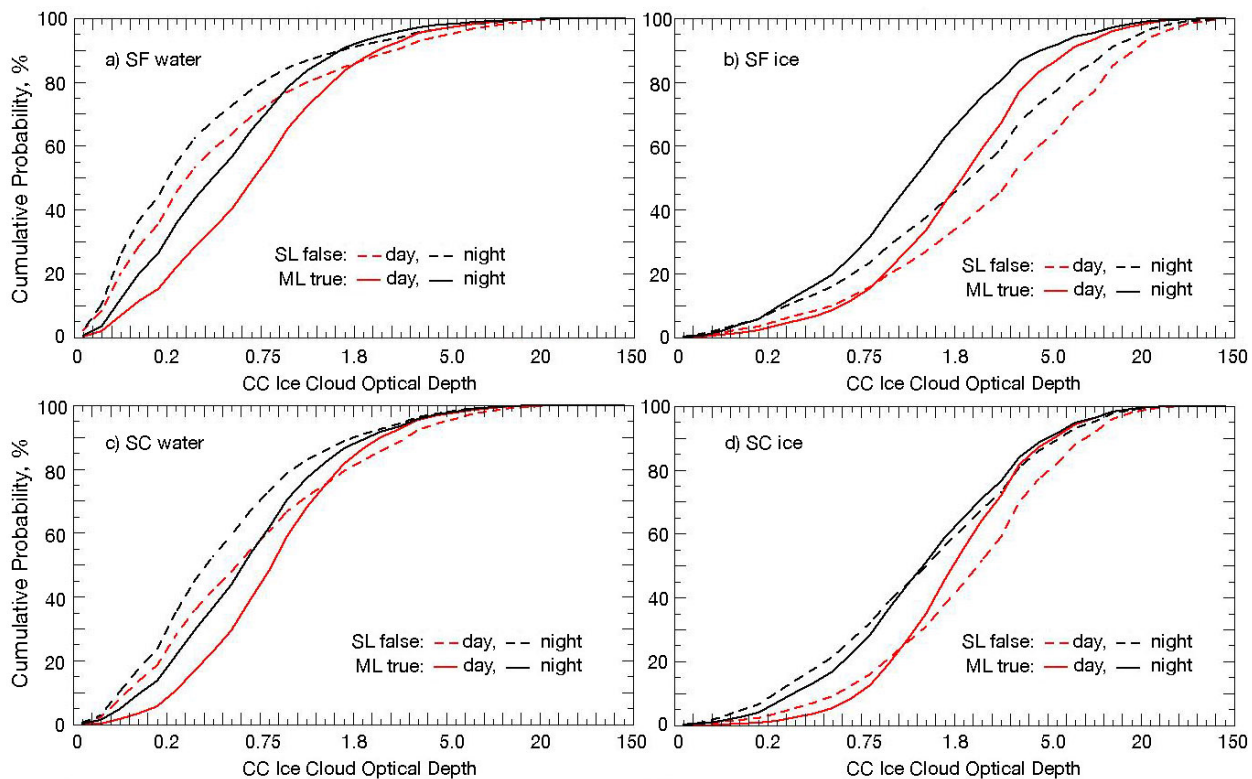
## **Identification of ice-over-water multilayer clouds using multispectral satellite data in an artificial neural network**

**Sunny Sun-Mack et al.**

*Correspondence to:* Sunny Sun-Mack (szedung.sun-mack-1@nasa.gov)

The copyright of individual parts of the supplement might differ from the article licence.

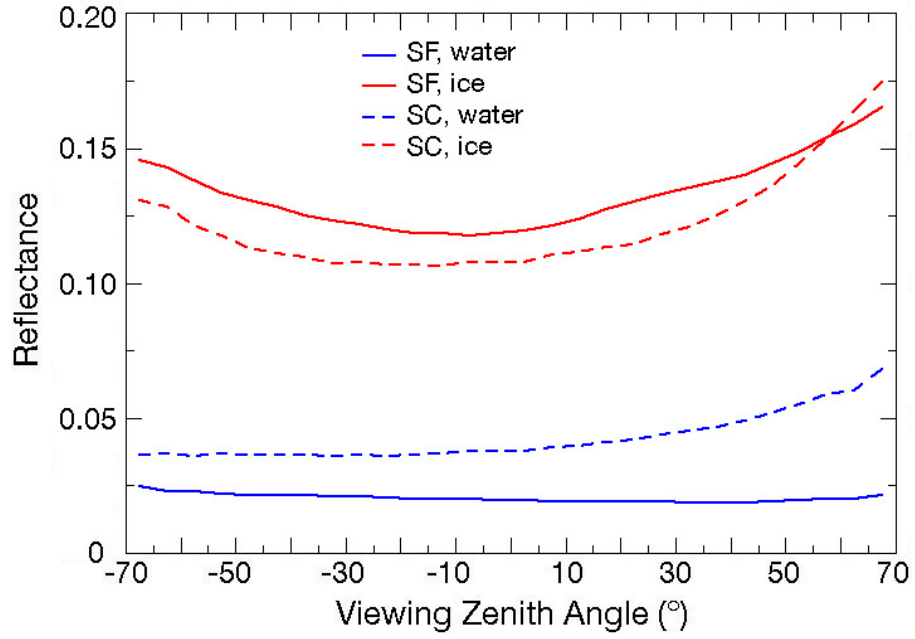
## Supplemental Material



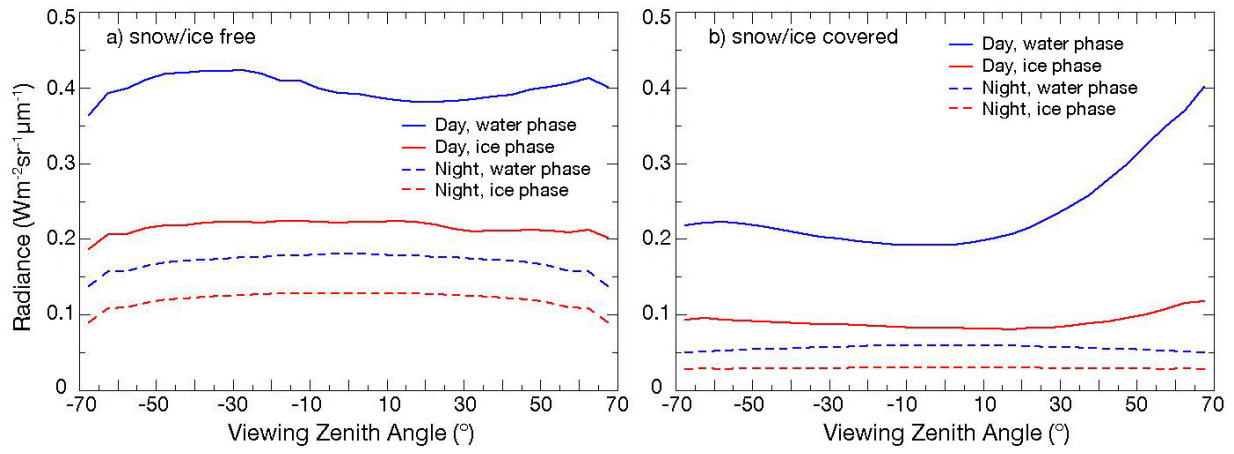
4  
5  
6  
7  
8  
9  
10

Fig. S1. Cumulative probability distributions of Aqua MODIS 2009 false SL and true ML clouds from MCANN as functions of upper-layer cloud optical depth for ice (left) and water (right) phase clouds over snow free (top) and snow/ice covered (bottom) surfaces. The major tick marks for the x-axes on the top panels are 0, 0.0025, 0.05, 0.1, 0.15, 0.2, 0.3, 0.4, 0.5, 0.6, 0.75, 0.9, 1.1, 1.3, 1.5, 1.8, 2.1, 2.5, 3, 4, 5, 6, 8, 10, 15, 20, 30, 40, 60, 80, and 150.

11  
12  
13  
14  
15



16  
17 Fig. S2. Global average Aqua MODIS 1.38- $\mu\text{m}$  reflectance as a function of viewing zenith angle  
18 for JAJO 2019.  
19  
20



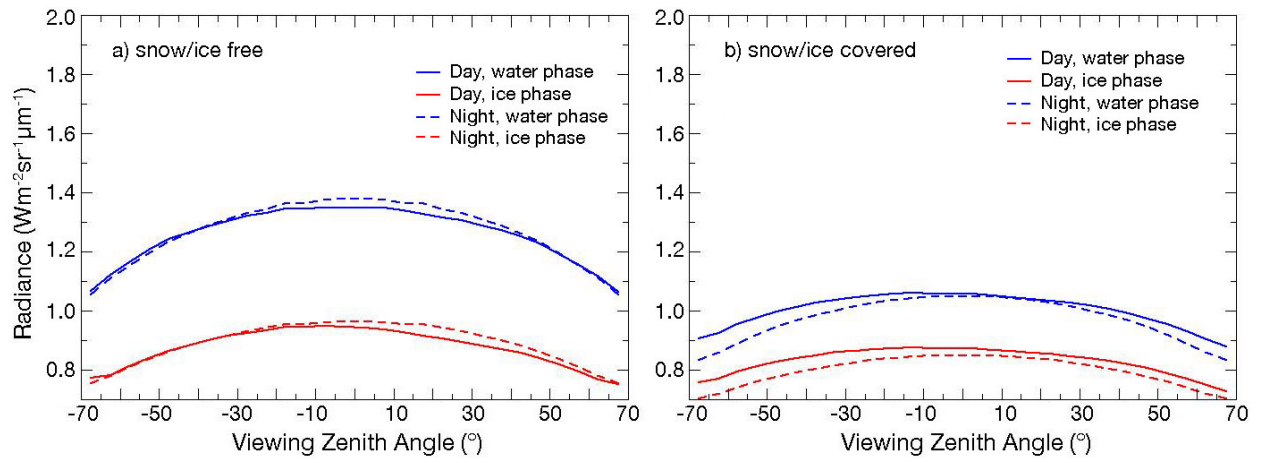
22

23

24 Fig. S3. Global average Aqua MODIS 3.75- $\mu\text{m}$  radiance as a function of viewing zenith angle for  
 25 JAJO 2019.

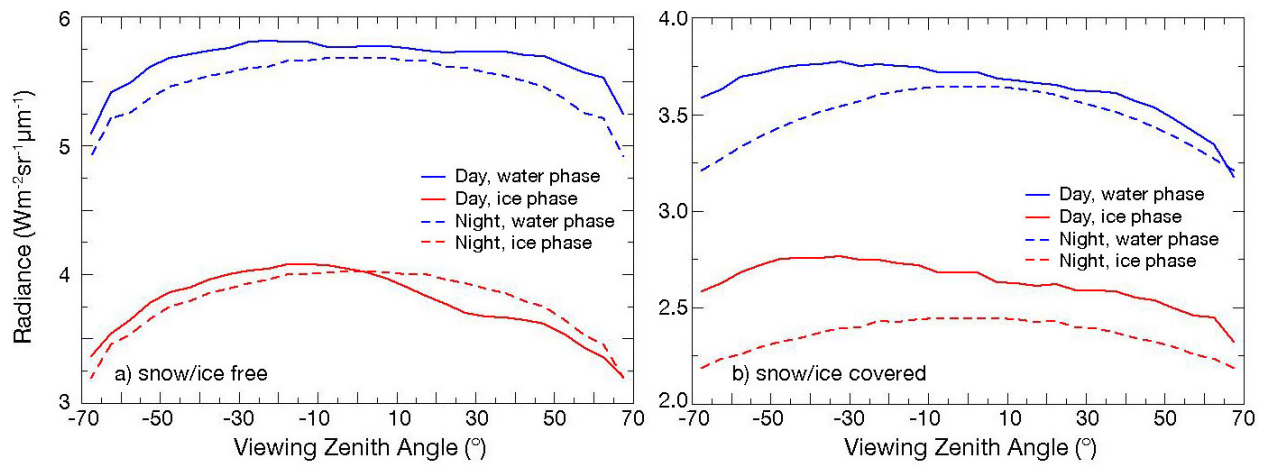
26

27



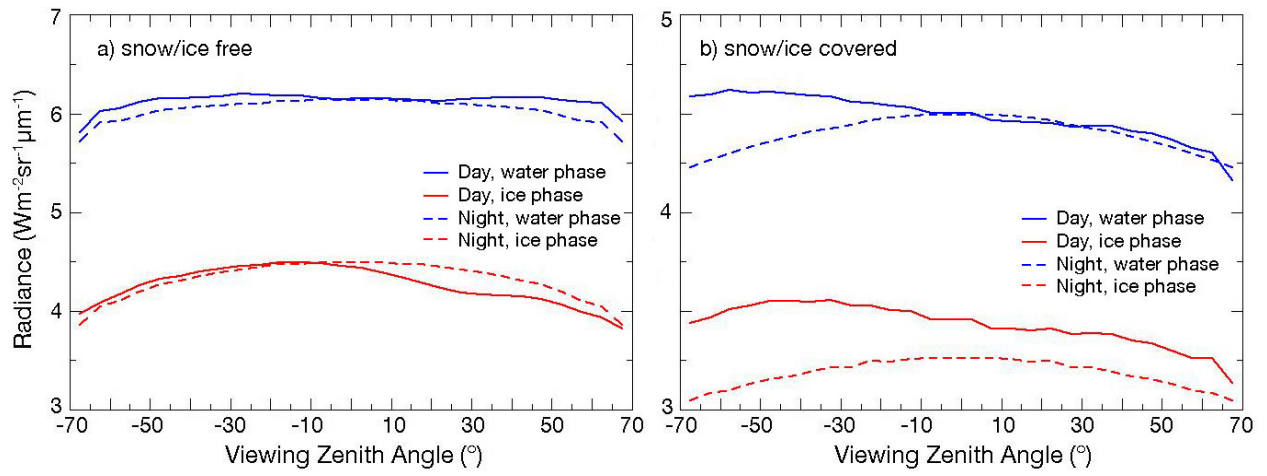
28  
 29  
 30  
 31  
 32

Fig. S4. Global average Aqua MODIS 6.70- $\mu\text{m}$  radiance as a function of viewing zenith angle for JAJO 2019.



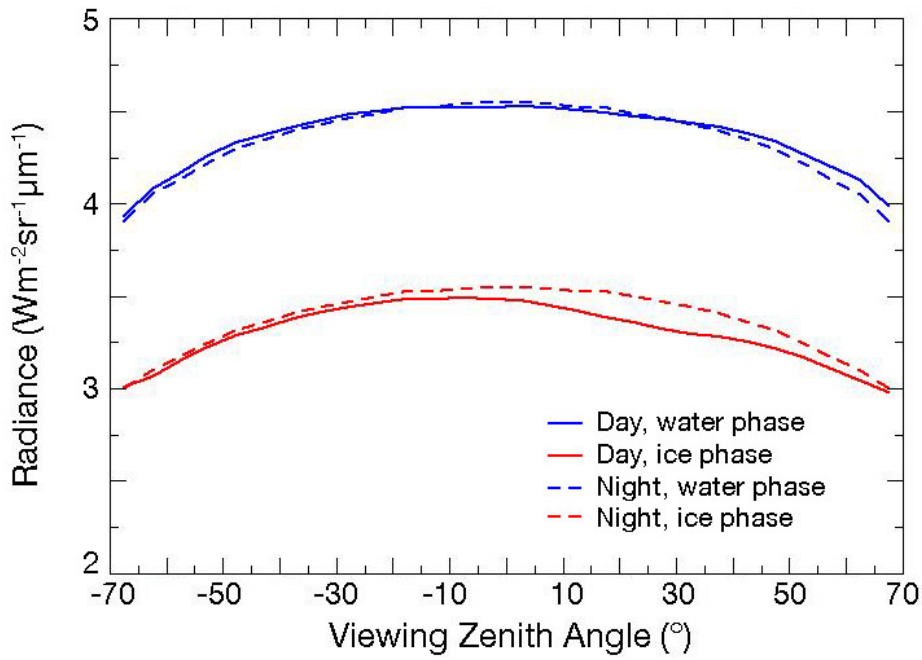
33  
 34  
 35  
 36  
 37  
 38

Fig. S5. Global average Aqua MODIS 8.55- $\mu\text{m}$  radiance as a function of viewing zenith angle for JAJO 2019.



39  
 40  
 41  
 42  
 43  
 44

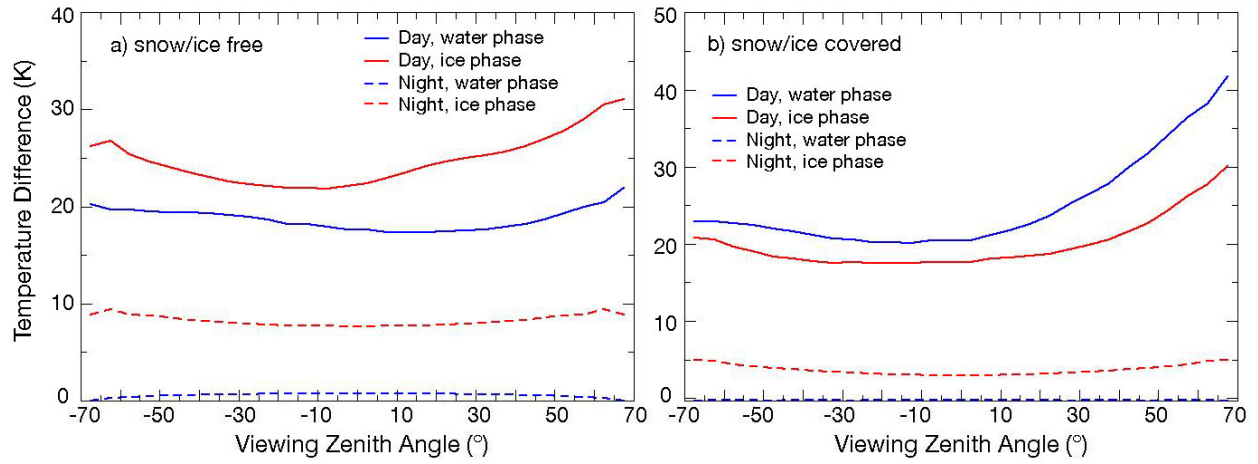
Fig. S6. Global average Aqua MODIS 11.9- $\mu\text{m}$  radiance as a function of viewing zenith angle for JAJO 2019.



45  
46  
47  
48  
49  
50

Fig. S7. Global average Aqua MODIS 13.3- $\mu\text{m}$  radiance as a function of viewing zenith angle for JAJO 2019 over snow/ice free surfaces.





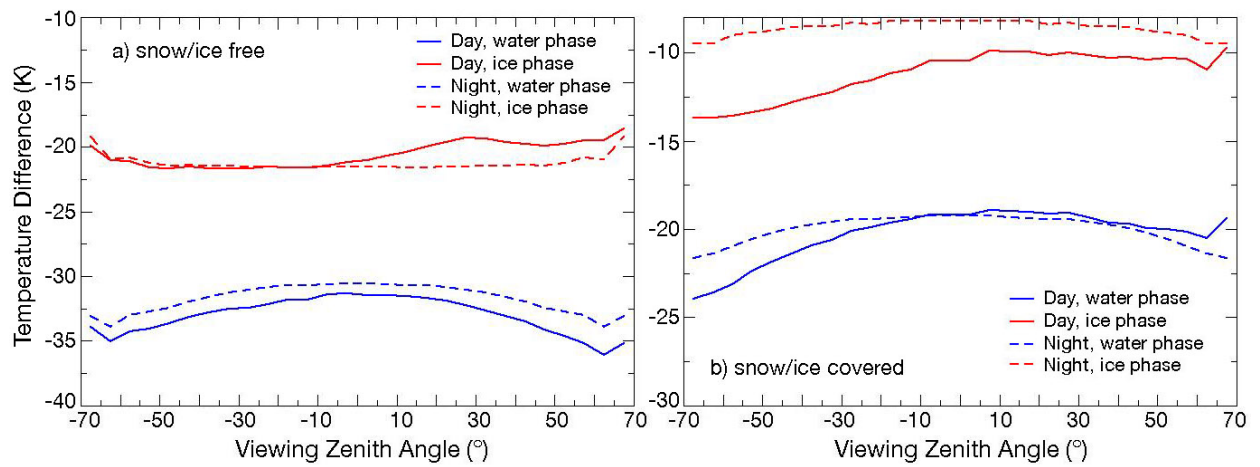
52

53

54 Fig. S8. Global average Aqua MODIS brightness temperature difference between 3.75- $\mu\text{m}$  and  
 55 10.8- $\mu\text{m}$  channels as a function of viewing zenith angle for JAJO 2019.

56

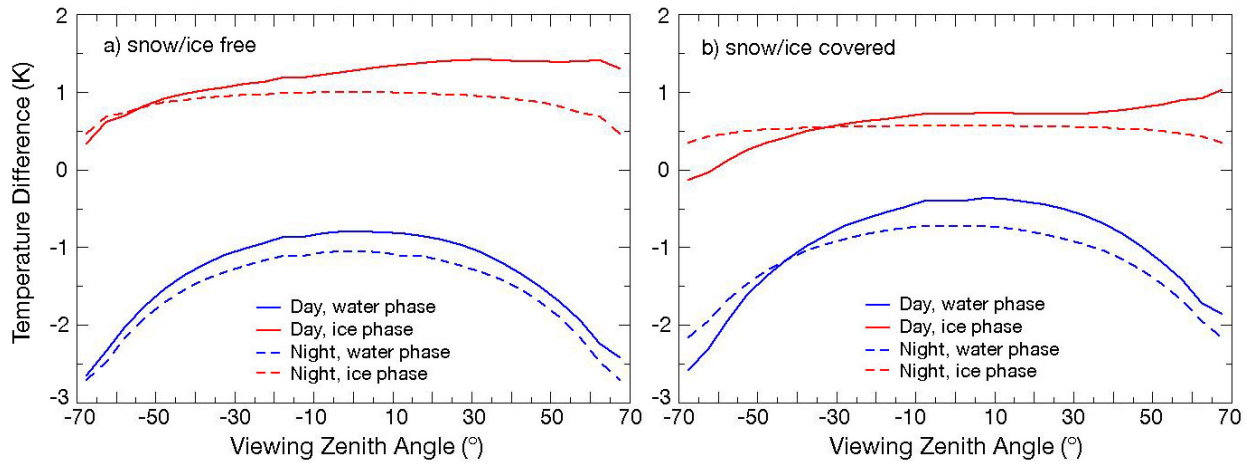
57



58  
 59  
 60  
 61  
 62  
 63

Fig. S9. Global average Aqua MODIS brightness temperature difference between 6.70- $\mu\text{m}$  and 10.8- $\mu\text{m}$  channels as a function of viewing zenith angle for JAJO 2019.

64

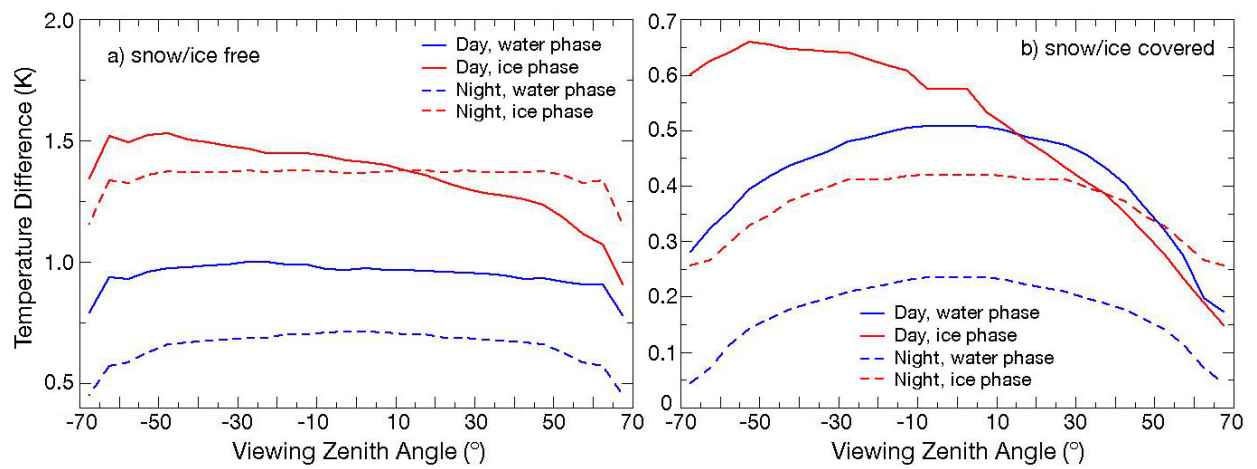


65

66

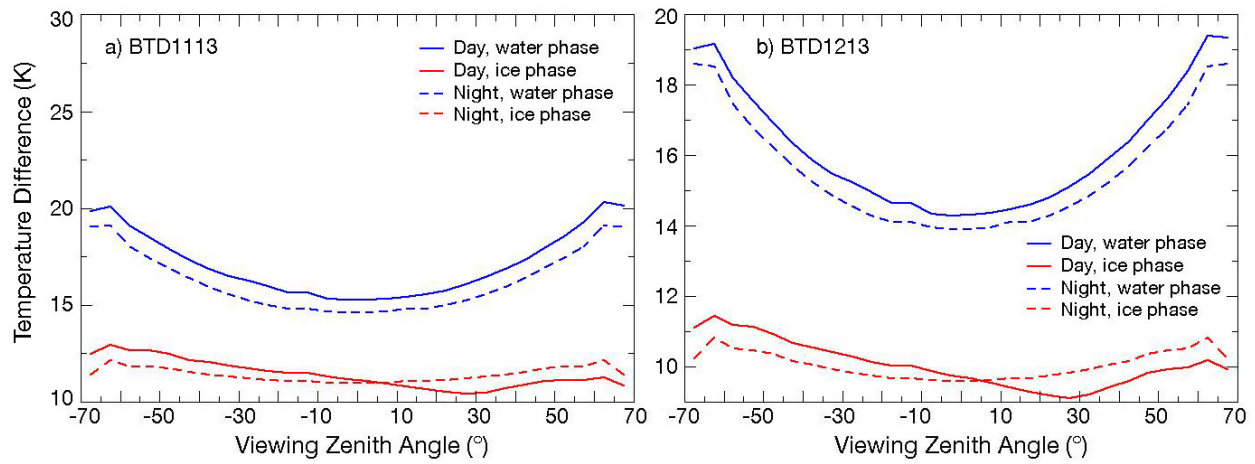
67 Fig. S10. Global average Aqua MODIS brightness temperature difference between 8.55- $\mu\text{m}$  and  
68 10.8- $\mu\text{m}$  channels as a function of viewing zenith angle for JAJO 2019.

69



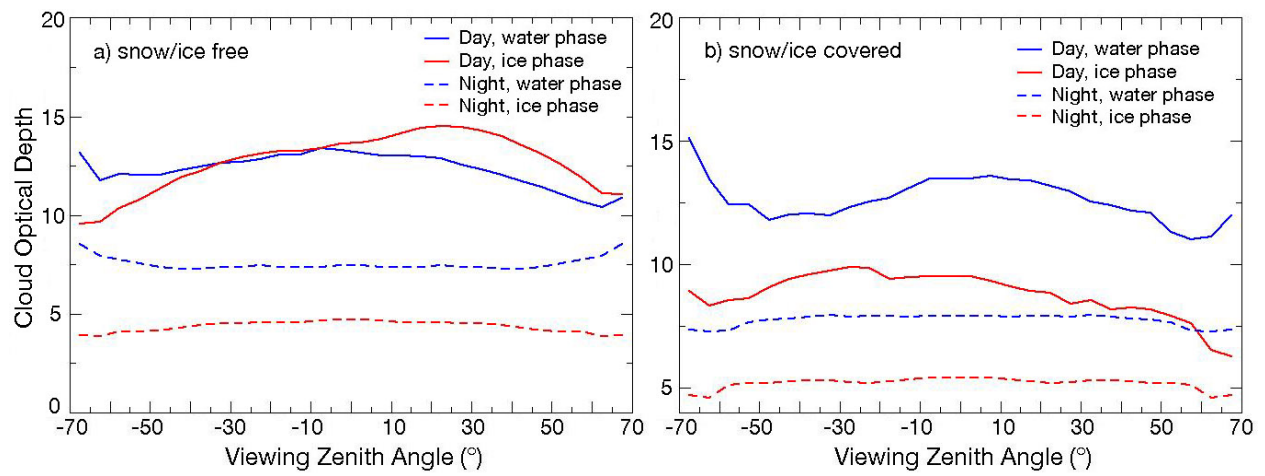
70  
 71  
 72  
 73  
 74  
 75

Fig. S11. Global average Aqua MODIS brightness temperature difference between 10.8- $\mu\text{m}$  and 11.9- $\mu\text{m}$  channels as a function of viewing zenith angle for JAJO 2019.



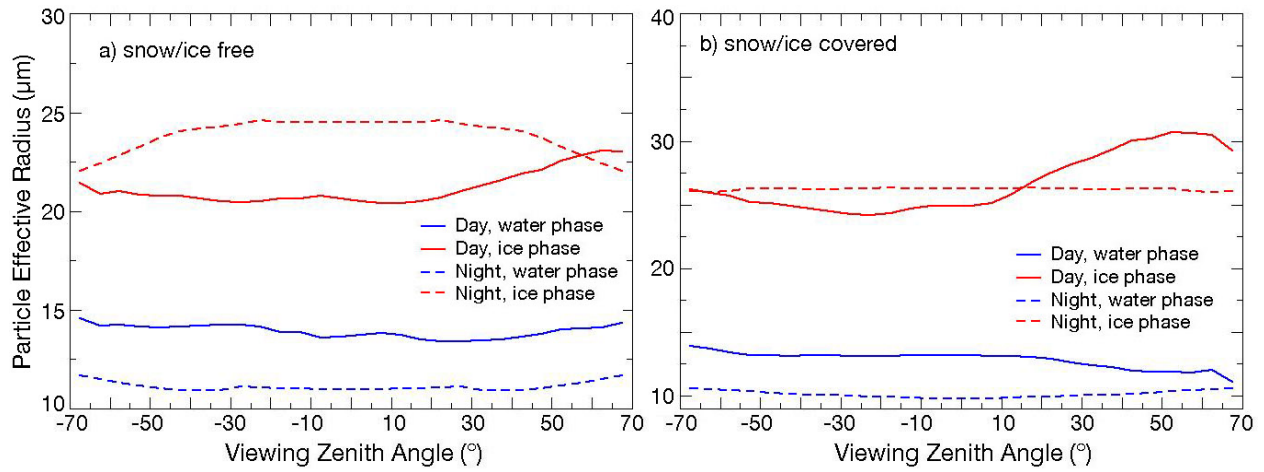
76  
 77  
 78  
 79  
 80

Fig. S12. Global average Aqua MODIS brightness temperature difference between (a) 10.8- $\mu\text{m}$  and 13.3- $\mu\text{m}$  and (b) 11.9- $\mu\text{m}$  and 13.3- $\mu\text{m}$  channels as a function of viewing zenith angle for JAJO 2019.



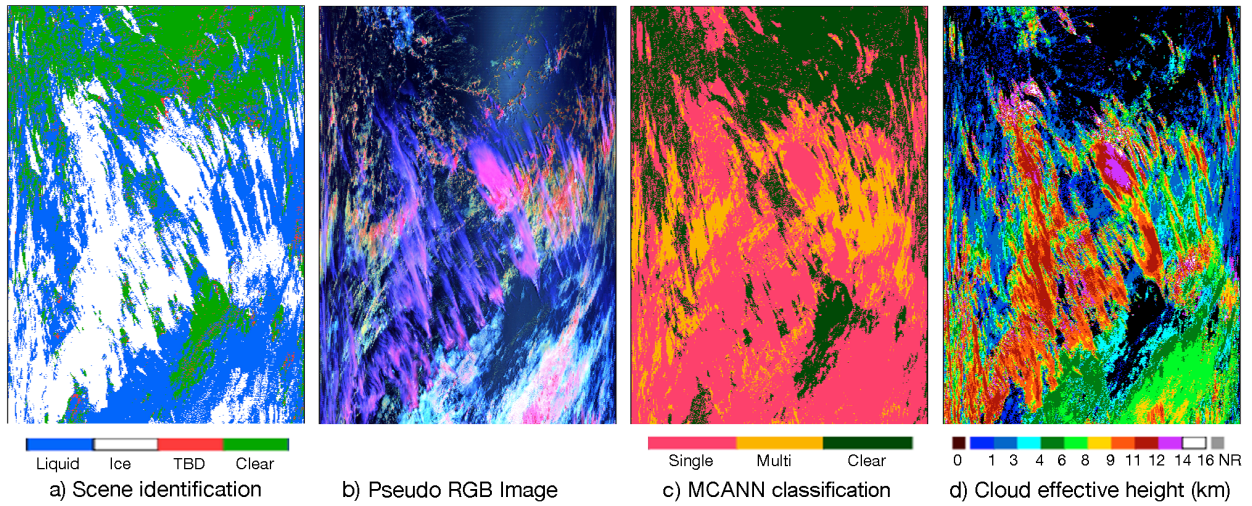
81  
 82  
 83  
 84  
 85  
 86  
 87

Fig. S13. Global average CM4 Aqua MODIS cloud optical depth as a function of viewing zenith angle for JAJO 2019.



88  
 89  
 90  
 91  
 92  
 93  
 94  
 95  
 96  
 97

Fig. S14. Global average CM4 Aqua MODIS cloud particle effective radius as a function of viewing zenith angle for JAJO 2019.



99

100 Figure S15. Cloud parameters derived from Aqua MODIS data between 1°N (top) and 13°N (bottom)  
 101 around 135°W, at ~22:35 UTC, 16 April 2019. (a) CM4 pixel scene classification, (b) Pseudocolor RGB  
 102 image, red: 0.64  $\mu\text{m}$  reflectance, green: BT<sub>37</sub>, green; blue: reverse BT<sub>11</sub>. (c) MCANN classification, and (d)  
 103 CM4 cloud effective height.

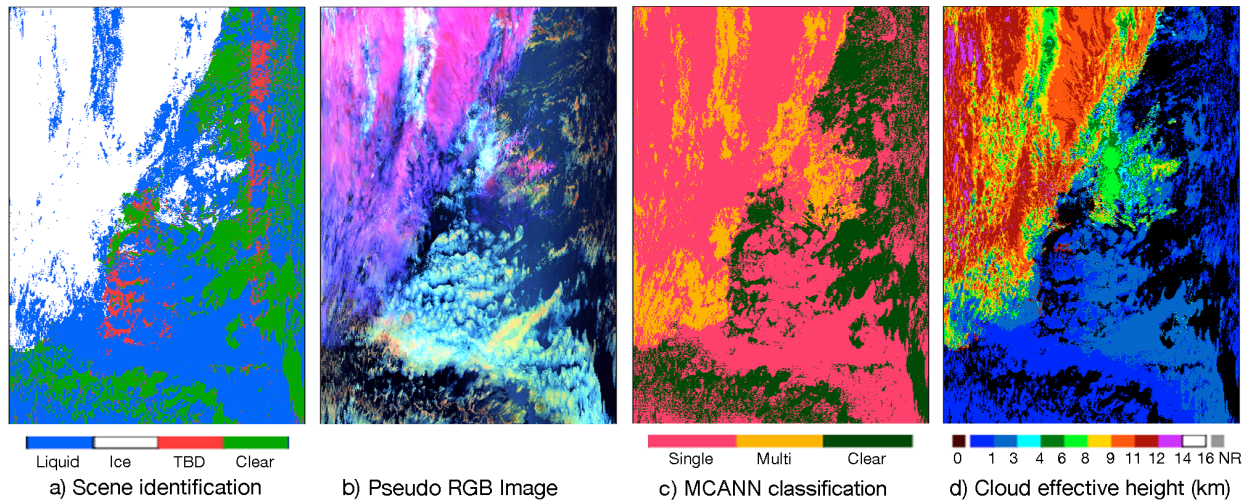
104

105



106

107



108 Figure S16. Cloud parameters derived from Aqua MODIS data between 29°N (top) and 17°N (bottom)  
109 around 140°W, at ~22:45 UTC, 16 January 2019. (a) CM4 pixel scene classification, (b) Pseudocolor RGB  
110 image, red: 0.64  $\mu\text{m}$  reflectance, green: BT<sub>37</sub>, green; blue: reverse BT<sub>11</sub>. (c) MCANN classification, and (d)  
111 CM4 cloud effective height.

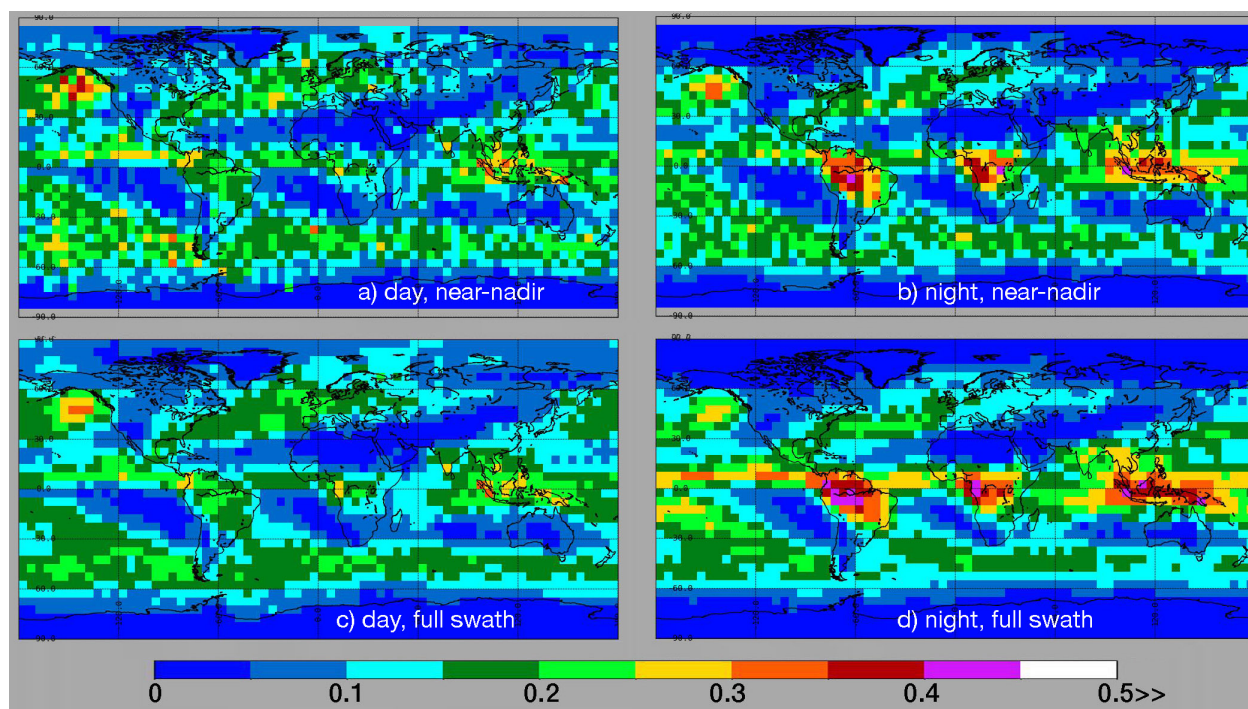
112

113

114

115

116



117  
 118  
 119  
 120 Fig. S17. Multilayer fraction of total cloud cover for JAJO 2013 using Aqua MODIS MCANN  
 121 retrievals (top) at near-nadir ( $-18^\circ < VZA < 3^\circ$ ), and (bottom) for all VZAs. Daytime on left,  
 122 nighttime on right.